David Elliott
Honours School of Microbiology
1999-2000
Supervised by Dr Pauline Handley

Detection of CshA Polypeptide on the Cell Surface of Oral Streptococci

David Elliott

ABSTRACT

The CshA polypeptide of *Streptococcus gordonii* DL1 has previously been shown to be a cell surface fibril of approximately 61 nm length, with adhesive and hydrophobic properties, required for colonisation of the oral cavity by *S. gordonii*. In this study a strains of different species of oral streptococci were screened for the presence of the N-terminal region of CshA by using an ELISA, which showed the CshA polypeptide to be widespread among the strains tested. CshA was detected on the surfaces of three strains of *S. gordonii*, two strains of*S. sanguis* and two strains of *S. oralis*, though not all members of these groups were confirmed to express CshA. The highest levels of cell surface CshA indicated by the ELISA were for two strains of *S. gordonii*. Transmission electron microscopy of negatively stained cells showed that all of the strains which produced a strong positive CshA ELISA result, had long and short cell surface fibrils (typically 160 nm and 60 nm long, respectively). Cell surface fibrils were individually measured from electron micrographs and plotted as histograms to reveal the most frequent range of lengths measured, from which an average length was determined. The anti N-CshA antiserum used in the ELISA was shown to bind to the short fibrils of these cells, by using an immuno-gold labelling technique in conjunction with negative staining and electron microscopy. The immuno-gold binding pattern supports the hypothesis that the CshA polypeptide is C-teminally anchored in the cell wall with its adhesive N-terminus distal to the cell.

INTRODUCTION

Streptococci are important colonisers of the oral cavity, and are typically involved in a commensal relationship with the host (Jenkinson and Lamont 1997). This relationship may shift to cause disease according to the prevailing conditions, and is further complicated by complex interactions with other members of the oral flora. Dental plaque is a complex multi-species biofilm attached to the surface of teeth, and is involved in the aetiology of periodontal disease and dental caries, which is the demineralization of tooth enamel resulting primarily from the production of acid by plaque bacteria (Marsh and Martin 1999).

The ubiquity of streptococci in the oral cavity and other sites throughout the body is largely due to their ability to adhere to host surfaces. The adhesion process between bacterium and substratum is generally considered to involve a sequence of events: first, the cell must be transported to the surface to which it is to adhere – this may be achieved by active motility or as a random collision. Close approach to the surface is usually prevented by electrostatic repulsion resulting from the negative charge of most bacterial cell surfaces. Hydrophobic forces counter this with an attractive force, and the bacterial cell is held in a loose association with the surface (adsorption), determined by the equilibrium between these non-specific interactions. In some cases electrostatic charge interactions may be sufficient to establish adhesion (Tellefson and Germaine 1986), but usually bacterial adhesins are considered necessary to achieve permanent attachment to a substratum, by specific interactions with receptors on the substratum (for a review see Hasty *et al* 1992). Logically there are two mechanisms by which this specific adhesin mediated adhesion may be achieved. The first is for the bacterial cell surface to contact the substratum so that cell surface adhesins (sometimes called nonpilus adhesins) can bind to substratum receptors. The second solution is for the bacterial adhesin to protrude from the cell surface so that only the bacterial adhesin is required to make close approach and contact with the substratum. Clearly the second solution is energetically more favourable for

cells approaching a surface, and this hypothesis is supported by observations of hair-like surface structures which have been implicated in adhesion for many bacterial species (for a review see Soto and Hultgren 1999). The terms used to describe these surface structures include fibrils, fimbriae, fibrillae, pili and curli. These terms are often used indiscriminately and without clear definition. In this report, the term “fibril” will be used to describe relatively short structures (50-400nm) composed of protein or glycoprotein and extending from the bacterial cell surface; the word “fimbriae” is used to describe longer structures composed of protein sub-units (from Handley *et al* 1999).

There are three broad sites to which bacteria may adhere in the oral cavity: teeth, mucosal epithelial cells, and the bacteria already coating these surfaces (Whittaker *et al* 1996). Cleaned teeth are rapidly coated with an acquired salivary pellicle of glycoproteins, which provides various binding sites for primary colonisers, including *Neisseria*, streptococci (including *S. sanguis, S. oralis, S. gordonii* and *S. mitis*) and actinomycetes. These primary colonisers are thought to bind to specific salivary molecules and to each other, forming a nascent surface to which further strains and species can adhere by co-aggregation to form dental plaque (Whittaker *et al* 1996). As early colonisers, the streptococci are extremely important in the process of plaque formation and the generation of dental caries.

In 1992 McNab and Jenkinson demonstrated that the CshA polypeptide of *S. gordonii* is a determinant of hydrophobicity and involved in coaggregation with *Actinomyces naeslundii*. Insertional mutagenesis has shown CshA and a similar polypeptide, CshB, to be required for colonisation of the murine oral cavity by *S. gordonii (*McNab *et al* 1994). The entire coding region of the c*shA* gene was cloned and the polypeptide structure was predicted based upon the deduced amino acid sequence (McNab *et al* 1994). The CshA polypeptide is predicted to be anchored to the cell wall by a carboxy terminal region, and has extensive amino acid repeat blocks comprising the central 60 % (1536 amino acids) of the sequence (total 2508 amino acids), probably arranged as an α-

helix. The N-terminal 878 amino acids are non-repetitive and include a leader sequence of 41 amino acids which is not present in the mature cell surface polypeptide. The remaining N-terminal region is proposed to be the major adhesion-mediating sequence, based upon the inhibition of adherence by antibodies (McNab *et al* 1996). Figure 1 shows the structure of CshA and highlights the N-terminal region used to generate antiserum (anti-N-CshA) for the adherence inhibition study. Identical anti-N-CshA provided by Prof. HF Jenkinson (Department of Oral and Dental Pathology, University of Bristol) was used in this study to investigate the distribution of cell surface expressed CshA polypeptide among oral streptococci.

Figure 1. Schematic representation of the CshA polypeptide of *S. gordonii* DL1.

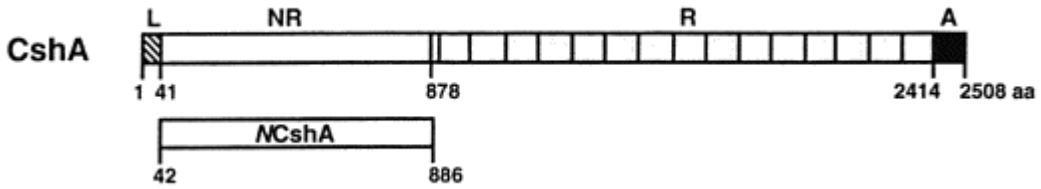

The CshA polypeptide consists of an N-terminal leader peptide (L), a non-repetitive region (NR), 13 amino acid repeat blocks (R), and a C-terminal anchor domain (A). (From McNab *et al* 1996). NCshA indicates the portion of the CshA polypeptide used to raise anti-N-CshA antiserum used in this study.

Anti-N-CshA antibodies have been shown to bind to the fibrils of *S. gordonii* DL1, and the CshA fibril length on the cell surface of this organism was found to be 60.7 +/- 14.5 nm (McNab *et al*, 1999). Heterologous expression of the CshA gene in *Enterococcus faecalis* JH2-2 endowed the bacterium with enhanced adhesion, auto-aggregation and hydrophobicity properties, along with the induction of 70.3 +/- 9.1 nm long fibrils on the cell surface which bind anti-N-CshA antibodies (McNab *et al*, 1999). Though CshA is a well characterised polypeptide, known to produce fibrils on *S. gordonii* DL1, and to facilitate adhesion and colonisation of murine oral surfaces, little is known about the distribution of CshA either in terms of its species range or its abundance and position the surface of individual cells. The aim of this study is to determine the amount of CshA polypeptide on the surfaces of oral

streptococci, including strains of *S. gordonii*, *S. sanguis*, and *S. oralis*. Following the determination of relative amounts of CshA on the cell surfaces of different strains, the strains will be analysed by negative staining to correlate the presence of CshA with structures on the cell surface. To locate the N-terminal region of the CshA polypeptide on the cell surface, cells will be immuno-gold labelled and negatively stained. Comparison of negatively stained and immuno-gold labelled negative stained cells will then allow comparison between cell surface fibrils and gold binding patterns to test the hypothesis that the N-terminal region of the CshA polypeptide forms the tips of fibrils distal from the cell surface.

MATERIALS AND METHODS

Organisms

A selection of oral streptococci (Table 1) were selected to be screened for expression of CshA by an enzyme linked immuno-sorbant assay (ELISA). The selected strains were mostly known to carry fibrils at various densities from electron microscopy studies (Handley *et al* 1985, Handley *et al* 1999, McNab *et al* 1999, Gibbons *et al* 1983) but the molecular composition of the fibrils is generally unknown.

Media

Bacteria were raised from frozen stocks in glycerol and grown on tryptone soya agar (Oxoid, Basingstoke, England); consisting of 15.0 gl^{-1} tryptone, 5 gl^{-1} soya peptone, 5.0 gl^{-1} sodium chloride, 15.0 gl^{-1} agar, with 0.3 % added select yeast extract (Sigma, St. Louis, USA) (TSAY). Cultures were incubated in a candle jar for 48 hours at 37^{o}C, before being moved to a refrigerator for storage at 4^{o}C, for up to four weeks before sub-culturing onto fresh TSAY. Overnight cultures were set up by inoculating approximately ten colonies into 20 ml universals containing tryptone soya broth with yeast extract (TSBY); 17.0 gl^{-1} pancreatic digest of caesin, 3.0 gl^{-1} papaic digest of soybean meal, 5.0 gl^{-1} sodium chloride, 2.5 gl^{-1} glucose, 0.3 % select yeast extract (Sigma, St. Louis, USA). The cultures were incubated static at 37^{o}C for 18 hours before harvesting by centrifugation.

Antisera and Buffer

Primary antiserum used for ELISA and immuno-gold labelling experiments was raised in rabbits against the N-terminal 844 amino acid residues of the mature CshA polypeptide of *S. gordonii* DL1 (anti N-CshA, see Figure 1), purified from *E. coli* (McNab *et al* 1996). The secondary antiserum used in gold labelling experiments was whole molecule anti-rabbit IgG developed in a goat, with a 10 nm gold conjugate (Sigma, St. Louis, USA).

Table 1. Oral streptococcal strains screened by ELISA for expression of surface-bound CshA-like polypeptide.

Strain	Notes	References
S.sanguis GW2	Dense long (150 nm) and short (75.3 nm) fibrils	1, 2
S.sanguis NCTC 10904	Surface properties unknown	
S.sanguis FC1	Fibrils present	3
S.sanguis nhm	Non-hydrophobic mutant of FC1, bald	3
S. gordonii PAR	Long (179 nm) and short (86.7 nm) fibrils	1, 2
S. gordonii JF2	Long (190 nm) and short (78.8 nm) fibrils	1, 2
S. gordonii GEO2	Fibrils (78.3 nm)	1, 2
S. gordonii LMH	Fibrils (71 nm)	1, 2
S. gordonii MJ2	Sparse fibrils (69.6 nm)	1, 2
S. gordonii CH2	Sparse fibrils (66.0 nm)	1, 2
S. gordonii DL1	Sparse fibrils of CshA (60.7 nm)	4
S. gordonii OB277	$CshA^-$, $CshB^-$ mutant of *S. gordonii* DL1	5
S. gordonii CR2b	Sparse fibrils (57.8 nm)	1, 2
S. crista NCTC 12479	Tufts of fibrils	1, 2
S. oralis KN	Sparse fibrils (53.2 nm)	1, 2
S. oralis EY3	Sparse fibrils (47.8 nm)	1, 2
S. oralis NCTC 11427	Surface properties unknown	
S. oralis 34	Surface properties unknown	
S. mitis PSH1b	Tufts of long (461 nm) and short (111.2 nm) fibrils	1, 2

References:

1. **Handley, *et al* YEAR?**
2. **Handley *et al* 1985**
3. **Gibbons *et al* 1983**
4. **McNab *et al* 1999**
5. **McNab *et al* 1994**

The buffer used during gold labelling experiments was 0.05 M Tris at pH 8.6 containing 1 % ovalbumin (Turkey egg grade V, Sigma, St. Louis, USA), 0.1 % gelatin (Sigma, St. Louis, USA), and 0.05 % Tween 20 (Oxoid, Basingstoke, England)

Enzyme Linked Immuno-Sorbant Assay (ELISA)

Anti-N-CshA was used as the primary antiserum in an ELISA (method modified from Holmes *et al* 1995), to give a measurement of the CshA expressed on the surfaces of the selected streptococcal strains.

Overnight cultures were harvested by centrifugation (4000g for 10 minutes at 4ºC), washed once in 10ml TNMC (1mM Tris-HCl at pH 8.0, 0.15 M NaCl, 0.1mM $MgCl_2$, 0.1mM $CaCl_2$) and suspended in TNMC at a cell density of $4x10^8$ cells/ml by adjustment of the OD_{600} to 0.40 - 0.42. The cell suspensions were dispensed onto NUNC Maxisorp microtitre plates and 24x50μl portions were dispensed for each strain to allow four replicates at three different primary antiserum and pre-immune antiserum dilutions. The plates were centrifuged for 5 minutes at 1500 rpm at room temperature and then held at 4ºC for 4-8 hours to allow binding of the cells to the plates. The solution was removed from the plates (by inverting and giving a sharp flick) and the wells washed once with 100μl TNMC to remove unbound cells. The plates were then blocked overnight with 100 μl TNMC containing 0.1 % BSA (bovine serum albumin) at 4ºC in order to block any remaining unbound binding sites on the plates. The blocking solution was removed and the wells washed twice with 100 μl TNMC containing 0.05 % Tween 20 (TNMC-Tween). After washing, 50μl of primary antiserum was applied to each well; each strain had four replicates of N-terminal antiserum and four replicates of pre-immune serum applied at three different dilutions (diluted in TNMC containing 0.1 % BSA to 1:1000, 1:2000 and 1:4000).

The plates were incubated at 37ºC for 60 minutes after the application of primary antiserum and then the solution was removed and the wells washed three times with 100 μl TNMC-Tween. The secondary antiserum (horse anti-rabbit conjugated to horse raddish peroxidase (HRP)) was applied next at 50 μl per well and diluted 1:1000 in TNMC containing 0.1 % BSA. The plates were again incubated at 37ºC for 60 minutes to allow antibody binding before removing the solution and washing the wells three times with TNMC-Tween. At this stage the cells have been attached to the plate, the primary antiserum

is bound to the CshA on the surface of cells and the secondary antibody along with the conjugated HRP is bound to the primary antibody. The final stage is the addition of 50 μl HRP substrate (Sigma P7288 [20 mg o-Phenylenediamine Dihydrochloride in 50 ml 0.1M citric acid-phosphate buffer at pH 5.0 + 20 μl 3.0 % H_2O_2]) per well for up to 30 minutes until colour develops. The reaction was stopped by addition of 50 μl 1.0 M H_2SO_4 to each well, and the plates are read in a spectrophotometer at 492 nm (Holmes *et al* 1995). The average pre-immune ELISA result for each serum concentration with each strain was subtracted from the N-CshA ELISA result and the standard deviation calculated (n=4); this treatment corrects for non-specific binding of the antiserum and gives an indication of the reproducibility of the data. *S. gordonii* OB277 is a mutant with $CshA^-$, $CshB^-$ phenotype (McNab *et al* 1994), and was included in the assay as a negative control.

Culture preparation for Electron Microscopy

Overnight cultures (18 hours) were set up and harvested by centrifugation at 3000 rpm, 4°C in a MSE Mistral 3000i centrifuge for 20 minutes. The harvested cells were washed three times in distilled water. After the final wash, cells were resuspended in water to form a dense milky suspension. For immuno-gold labelling the bacterial suspensions were washed and suspended in buffer instead of water, to block non-specific binding of antiserum. The gold labelling buffer was 0.05 M Tris at pH 8.6 containing 1 % ovalbumin (Sigma, St. Louis, USA), 0.1 % gelatin, and 0.05 % Tween 20.

Negative staining

To reveal the surface structures of the bacteria in the electron microscope, specimens were negatively stained with methylamine tungstate (Agar Scientific, Essex, England). The bacterial suspensions were mixed on formvar (2 % w/v solution in chloroform) and carbon coated 400 mesh copper grids (Athene G204) with an equal volume of 1% (w/v) methylamine tungstate in distilled water adjusted to pH 6.5. The grids were plasmaglowed (in a Fisons PT7150 RF Plasma Barrel Etcher) to render the surface hydrophilic and aid spreading of the negative stain.

Immuno-gold labelling

To show the distribution of CshA polypeptide on the cell surface by electron microscopy, cells were immuno-gold labelled, following the procedure of McNab *et al* (1999). Briefly, specimens were treated with anti N-CshA antibodies raised in a rabbit (as used in the ELISA), and a secondary goat-anti-rabbit gold-conjugate was applied to specifically label the CshA on the cell surface with 10 nm gold particles (Figure 3).

Figure 3. CshA Immuno-Glold Labelling Principle

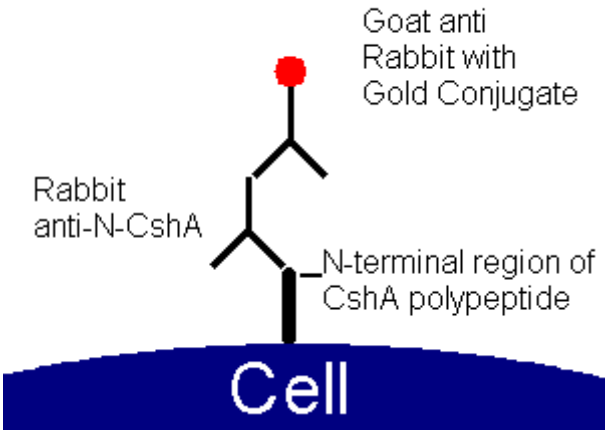

The primary antiserum (rabbit anti-N-CshA) binds to the N-terminal region of the CshA polypeptide. After washing, the secondary antiserum (goat-anti-rabbit gold conjugate) is applied, and binds the attached primary antiserum, thereby labelling the CshA polypeptide with a gold particle. Not to scale.

The gold labelling procedure was performed by the transfer of grids along a line of reagent drops, each of approximately 25 μl. Bacteria were first added to the grids in the same way as for negative staining, and then the grids were immuno-gold labelled by transfer from drop to drop with tweezers as shown in Figure 4. After an initial five minute wash in buffer, the grids were incubated for thirty minutes with the primary anti N-terminal-CshA antiserum, followed by five washes in buffer for one minute each, and then a further thirty minutes incubation in goat-anti-rabbit gold conjugate. The sequence was completed by five washes of one minute duration in water (slightly alkaline), and negative staining with methylamine tungstate. Gold labelling was performed in

duplicate, and with a negative control in which the primary antiserum was replaced with buffer to reveal any non-specific binding by the gold-conjugate. A positive control was also employed when labelling *S. sanguis* nhm, by running an organism known to become labelled (*S. sanguis* FC1) in parallel to confirm that any failure of the organism to become labelled is not due to failure of the labelling process.

Figure 4. Immuno-gold negative staining process

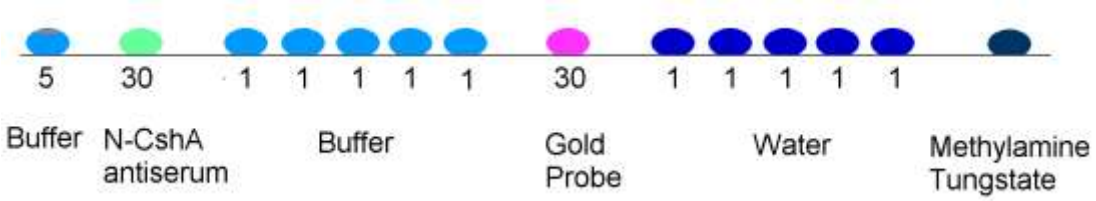

START (numbers indicate incubation time (minutes) for each stage) **FINISH**

Gold labelling of cells was achieved by applying a bacterial suspension to a specimen grid, and floating the grid on the succession of reagent drops shown. The grid was not allowed to dry out during the process.

Fibril Length Measurements from Electron Micrographs

On any given cell there may be more than one class of fibril, of partial or full extension. This variation presents a problem in the measurement of individual classes of fibril for characterisation. Previous attempts at fibril measurement (Handley *et al* 1985) involved the observation and measurement of a "fringe" produced around the cell surface by the extended fibrils, therefore any fibrils at partial extension do not interfere due to selection of the longest fibrils from each class. A similar method was used in this experiment, but it was considered more accurate and objective to take measurements of individual fibrils, and then re-create the fringe from the data to determine the full fibril length. To avoid unnecessary time consuming measurements, only fibrils at or near full length (as determined by observation of the fringe and other fibrils) were measured. In most cases more than one distinct class of fibril-like structure were present, but the quite variable length of the longer structures did not usually produce a clear fringe or typical length, so all long structures were measured (Figure 5). Figure 5 shows a hypothetical model of the fibril

lengths found on a typical cell surface; it is assumed that fibrils do not immediately appear on the cell surface at full length, but gradually extend during maturation of the cell wall. Apparent extension of a structure of fixed length may occur if it is anchored into the peptidoglycan of the cell wall, which continuously migrates outwards from the cell as new cell wall is laid down near the cell membrane. If there is a fixed maximum length for a given fibril class (e.g. monomeric fibrils composed of a single polypeptide), then no further extension will occur and there will be an accumulation of fully extended fibrils on the cell surface, producing a fringe. Structures of no fixed maximum length (e.g. fimbriae composed of subunits) would be expected to produce a variable profile without the accumulation of a specific length structure or production of a fringe.

Fibril lengths were measured from electron micrographs of approximately fifty negatively stained cells for each strain, using an eyepiece and graticule. Individual fibrils were selected for measurement, only if their length could be clearly seen; fibrils suspected to have originated from behind the cell surface on the photograph, or deep within the cell wall, were ignored to avoid measuring only part of the fibril length. Fibrils were usually not visible on immuno-gold labelled cells, so all gold particles beyond the cell surface were measured to the inner edge of the gold particle. This approach ensures that the results are unbiased by selective measurement, and allows statistical analysis to be used to reveal the most frequent gold distance from the cell surface.

Analysis of Fibril and Gold Distance Measurements

For comparison of fibril length and gold distance from the cell surface, cells from a single broth were simultaneously negatively stained and gold labelled to eliminate any chance of batch to batch variation in fibril length. The measurements were ranked and individually plotted to allow a visual assessment. Histograms were also plotted to reveal the distribution of results and highlight the most common range within which measurements lie.

Figure 5. Hypothetical model of fibril extension and selection of fibrils for measurement.

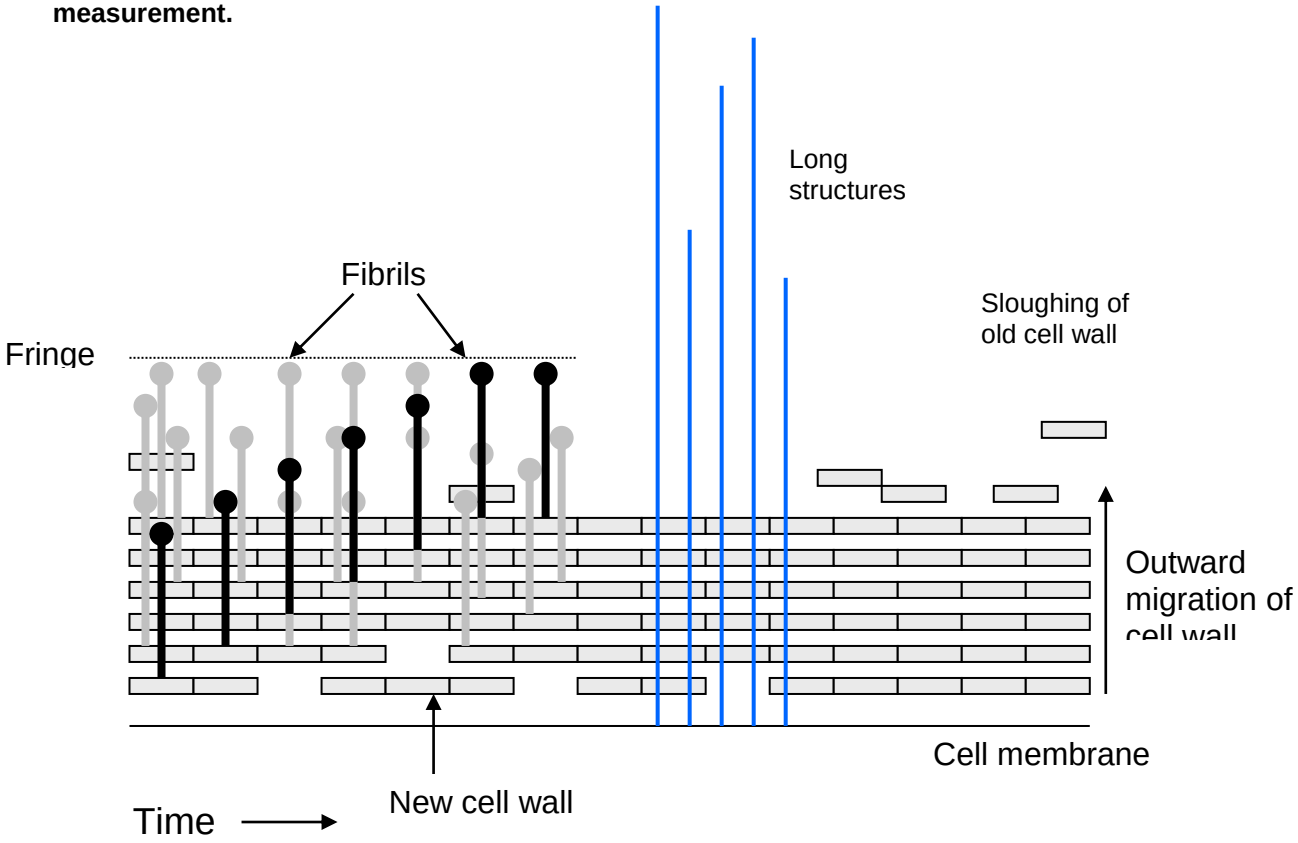

A section of cell wall is shown where new cell wall material (i.e. peptidoglycan) is being laid down just outside the cell membrane, therefore necessitating the outward migration of older cell wall material. Fibrils are shown attached to the newest layer of peptidoglycan, and migrate outwards with the wall as new cell wall is laid down beneath. The extension of a single fibril over time is highlighted in black, and other fibrils are shown in grey to illustrate the generation of a fringe. Fibrils extending to, or near to the fringe were selected for measurement. Longer structures are shown as thin lines attached to the cell membrane, though the attachment point of these structures is unknown. The variable length which longer structures extend from the cell wall is proposed to result from the variable length of the structures, all structures longer than the short fibril class were measured. Cell wall diagram modified from Niedhardt *et al* (1990).

RESULTS

Detection of CshA N-terminal region on oral streptococci by ELISA

Two separate ELISA experiments were required to accommodate all of the strains, and *S. gordonii* DL1 was used as an internal positive control to standardise the two sets of data. The ELISA results are shown in Figure 6, ranked and expressed as a percentage of the maximum absorbance result (0.361 for *S. gordonii* DL1).

Increased absorbance (A_{492}) is due to the production of a yellow colour upon development of the ELISA, and is the signal used to report the reactivity of the test strain with the N-CshA primary antiserum used. The ELISA produced a range of absorbance values, with two strains giving a high absorbance, six intermediate strains, and ten strains producing little or no increase in absorbance (Figure 6). The highest absorbance was produced by *S. gordonii* DL1. Two other strains of *S. gordonii* (MJ2 and PAR) also gave a high or intermediate absorbance but the other five *S. gordonii* strains tested gave little or no ELISA reaction. All three *S. oralis* strains tested gave a positive reaction, and two of the four *S. sanguis* strains (NCTC 10904 and FC1) gave strong ELISA reactions, while the other two gave only low reactions. *S. crista* 12479 produced a low absorbance and *S. mitis* PSH1b produced no change in absorbance, as did the negative control *S. gordonii* OB277.

Apart from the two highest ELISA reacting strains, *S. gordonii* DL1 and *S. gordonii* MJ2 which gave results of 100 % and 81 % respectively, the majority of clear positive results were in the range 30 – 50 %.

The pattern of absorbance results (Figure 6) allows the strains to be grouped as shown in Table 2. *S. mitis* PSH1b, *S. gordonii* OB277 (-ve control), *S. gordonii* CH2, *S. gordonii* JF2, *S. gordonii* LMH and *S. gordonii* CR2b all gave an absorbance result within 1 standard deviation of zero. The four other strains in the low reactivity group (*S. crista* 12479, *S. sanguis* GW2, *S. sanguis* nhm, *S. gordonii* GEO2) produced a low but definite reaction,

indicating that CshA may be present on the cell surface. All of the other strains gave clear positive results (i.e. CshA clearly detected on the cell surface).

Figure 6. Ranked N-CshA ELISA data showing the percentage of maximum absorption produced by each strain

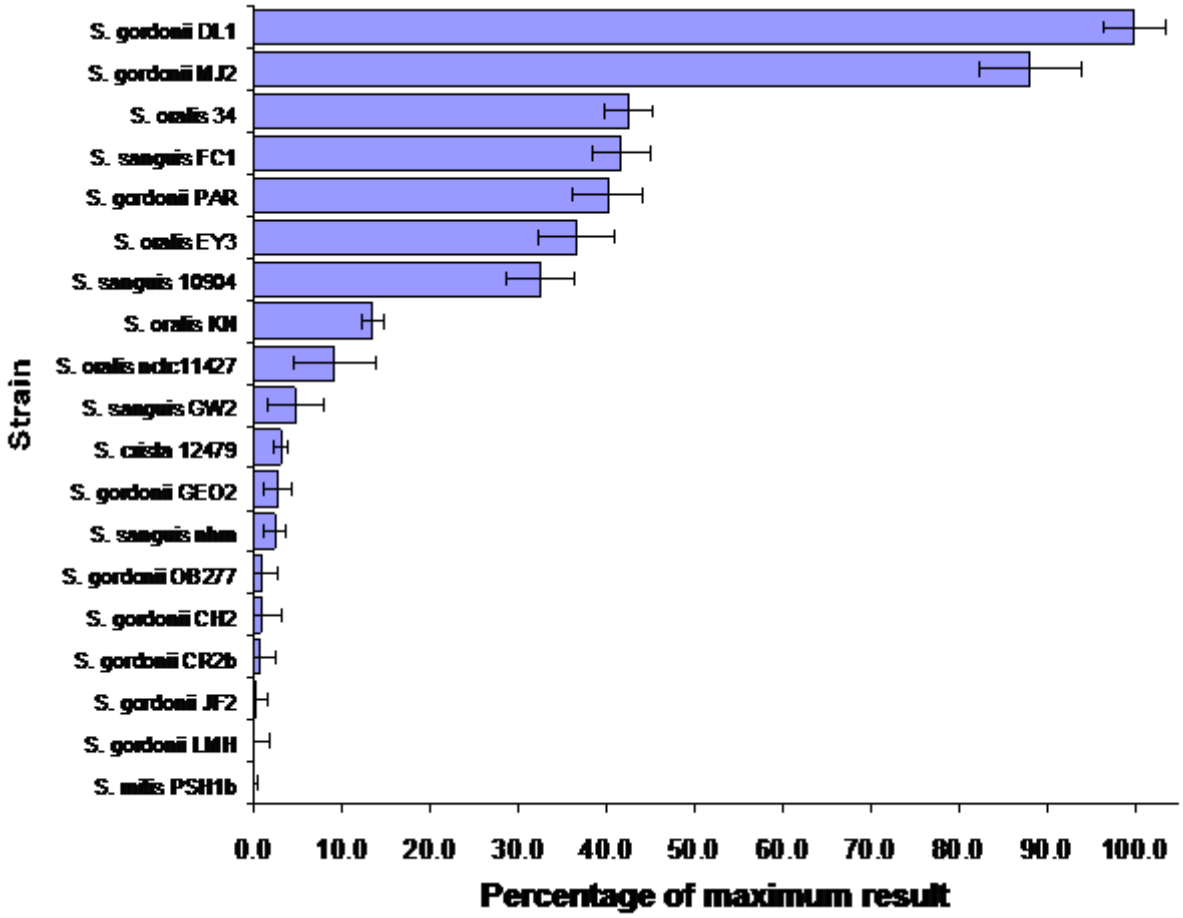

N-CshA ELISA results for oral streptococci are ranked and expressed as a percentage of the maximum reactivity. Error bars represent 1 standard deviation (n=4).

The clear positive N-CshA antiserum reacting strains included three *S. gordonii* strains, three *S. oralis* strains, and two *S. sanguis* strains. The eight *S. gordonii* strains tested showed variable reactivity from one to another. *S. sanguis* FC1 gave a typical intermediate reaction, but its non-hydrophobic mutant, *S. sanguis* nhm, gave a low to zero absorbance result.

Table 2. ELISA Reactivity groups for oral streptococci probed with anti-N-CshA antiserum

ELISA reactivity groups (percentage of maximum reactivity)			
Low (<5 %)	**Quite low (5–15 %)**	**Medium (15-50 %)**	**High (>50%)**
S. mitis PSH1b	*S. oralis* KN	*S. oralis* 34	*S. gordonii* DL1
S. crista 12479	*S. oralis* NCTC 11427	*S. oralis* EY3	*S. gordonii* MJ2
S. sanguis GW2		*S. sanguis* NCTC 10904	
S. sanguis nhm		*S. sanguis* FC1	
S. gordonii OB277		*S. gordonii* PAR	
S. gordonii CH2			
S. gordonii JF2			
S. gordonii GEO2			
S. gordonii LMH			
S. gordonii CR2b			

Oral streptococci are grouped according to the amount of CshA detected on the cell surface by an ELISA specific for the N-terminal region of the CshA polypeptide.

Analysis of Cell Surface Structures and N-CshA antiserum binding by Electron Microscopy

The medium and high ELISA reactive strains were selected for examination by electron microscopy to detect CshA. Negative staining was used to reveal surface structures, and immuno-gold labelling followed by negative staining, was used to identify structures having epitopes antigenically related to the N terminal region of the *S. gordonii* DL1 CshA polypeptide.

Negative staining of cells produced clear pictures of the cell surface enabling visualisation and measurement of the fibrils from each strain. Fibrils often appeared to be clumped together, but in some instances, individual fibrils could apparently be seen as very fine projections (Figure 7). Globular ends were occasionally observed on fibrils, but the ends of most fibrils had no obvious “end” structure. The pictures obtained from immuno-gold labelled cells clearly showed the cell wall and gold particles, allowing measurements to be taken, but in most cases the fibrils were not visible. Where fibrils could be seen, they were sometimes not labelled with gold particles. Where gold labelled fibrils could be seen, the gold typically adhered close to the fibril tip and the fibrils were often not normal to the cell surface, or the gold particle

bound to the tip of two or more fibrils held in a triangular arrangement (Figure 8). If no fibril can be seen in association with a particular gold particle, then both of these situations result in the gold particle being measured at a shorter distance than if it were bound to a single fibril normal to the cell surface (Figures 7 & 8).

All fibrillar strains had short fibrils similar to those previously described for *S. gordonii* DL1 and *Enterococcus faecalis* JH2 transformed with the *CshA* gene of *S. gordonii* DL1 (McNab *et al* 1999). In addition, all of these strains had longer structures protruding from the cell surface. Both types of structure could be seen emerging from the cell wall, often with a distinct protrusion of the wall at the base of the structure.

Distribution of fibrils and gold particles on the cell surface

The density of fibrils on the cell surface was greatest at the poles of cells, and particularly on the outermost pole of cells at the ends of chains of cells (Figure 7). Though fibril density was greatest at cell poles, fibrils were always observed to be peritrichously arranged on the cell surface, and not arranged in distinct tufts. Gold particles preferentially bound to the poles of immuno gold labelled cells.

***S. sanguis* FC1 and *S. sanguis* nhm.** *S. sanguis* nhm is a non-hydrophobic mutant of *S. sanguis* FC1 isolated by Gibbons *et al* (1983) using a hydrophobic enrichment technique. This mutant appeared completely bald in the electron microscope (not shown) with no fibrils or longer structures present, confirming the observation of Gibbons *et al* (1983) that the mutant possesses no fimbriae. These mutant cells also failed to become labelled with gold.

At least two distinct structures could be seen protruding from the surface of *S. sanguis* FC1 (figure 7), these were fibrils and longer hair-like protrusions, which will be described as “long structures”.

Figure 7. Electron micrograph of negatively stained *S. sanguis* FC1

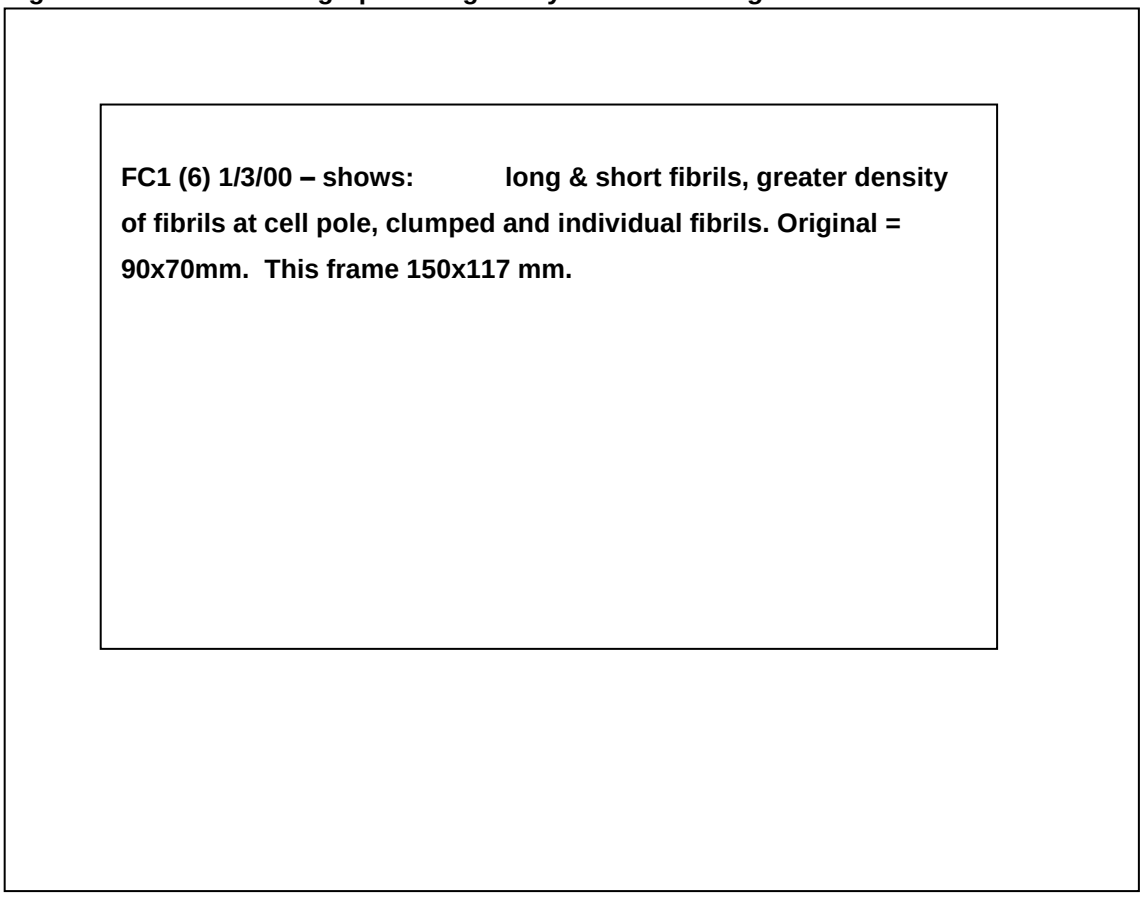

Negatively stained *S. sanguis* FC1, showing long and short fibrils predominantly at the cell pole. Most structures are clumped together, but some fine hair-like individual structures are visible (arrow).

Figure 8. Electron micrograph of immuno-gold labelled, negatively stained *S. sanguis* FC1

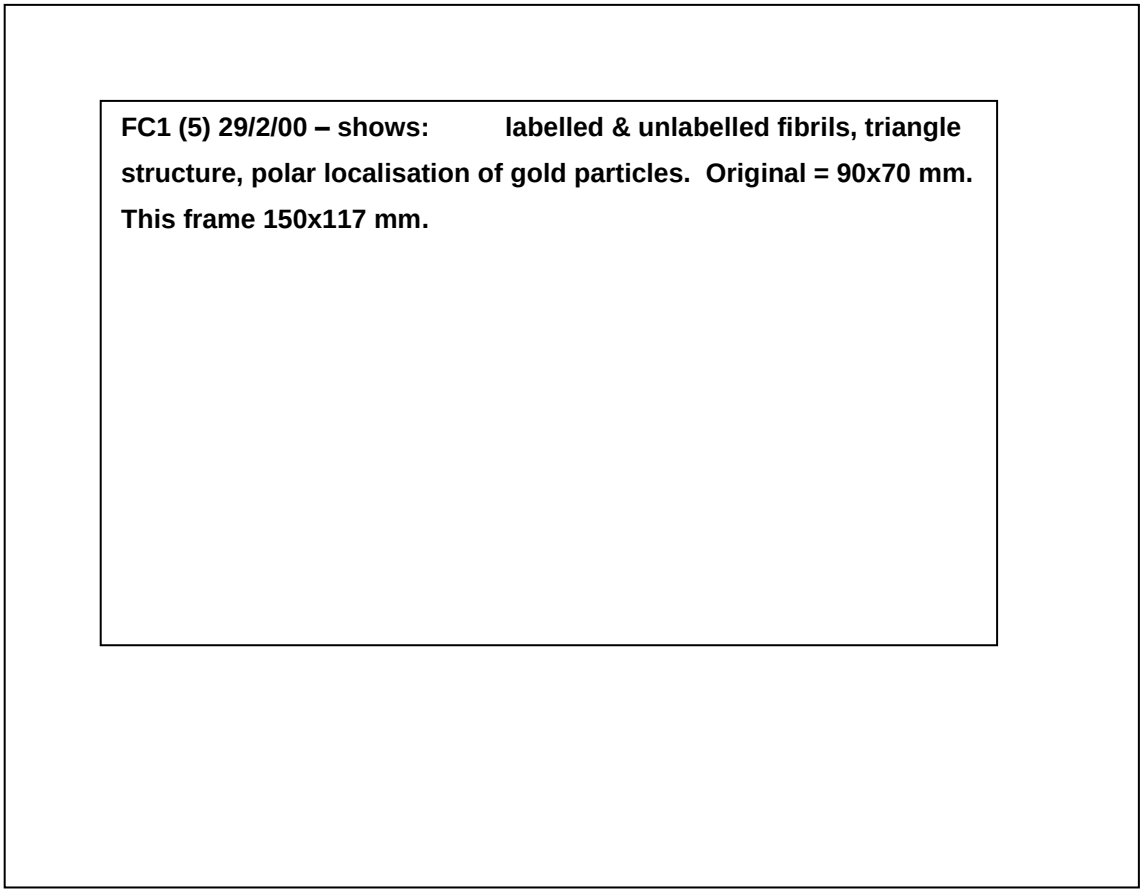

Gold labelled *S. sanguis* FC1, showing the majority of gold particles bound at the pole of the cell. In most cases the structure to which gold particles are adhered can not be seen, but two or more fibrils can be seen with a single gold particle at their tips, forming a triangular arrangement (arrow), and two distinct fibrils which appear to have originated from behind the cell surface can be seen with gold particles at their tips (arrow)

***S. sanguis* NCTC 10904.** Negative staining of *S. sanguis* NCTC 10904 revealed a surface similar to that of *S. sanguis* FC1, having fibrils and a high proportion of longer structures (figure 9).

Figure 9. Electron micrograph of *S. sanguis* NCTC 10904

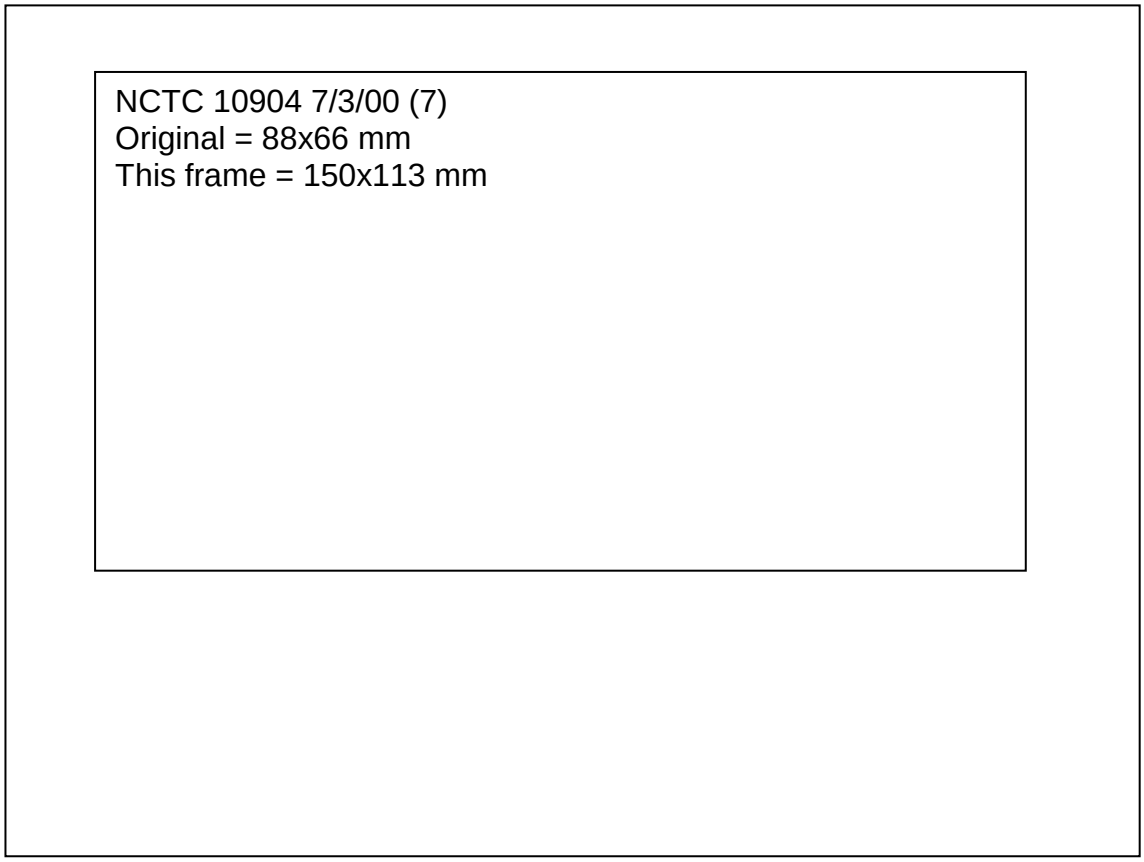

The cell surface of *S. sanguis* NCTC 10904 is dominated by long structures

***S. gordonii* PAR.** Both fibrils and longer structures were observed on the surface of *S. gordonii* PAR (figure 10).

Figure 10. Electron micrograph of *S. gordonii* PAR

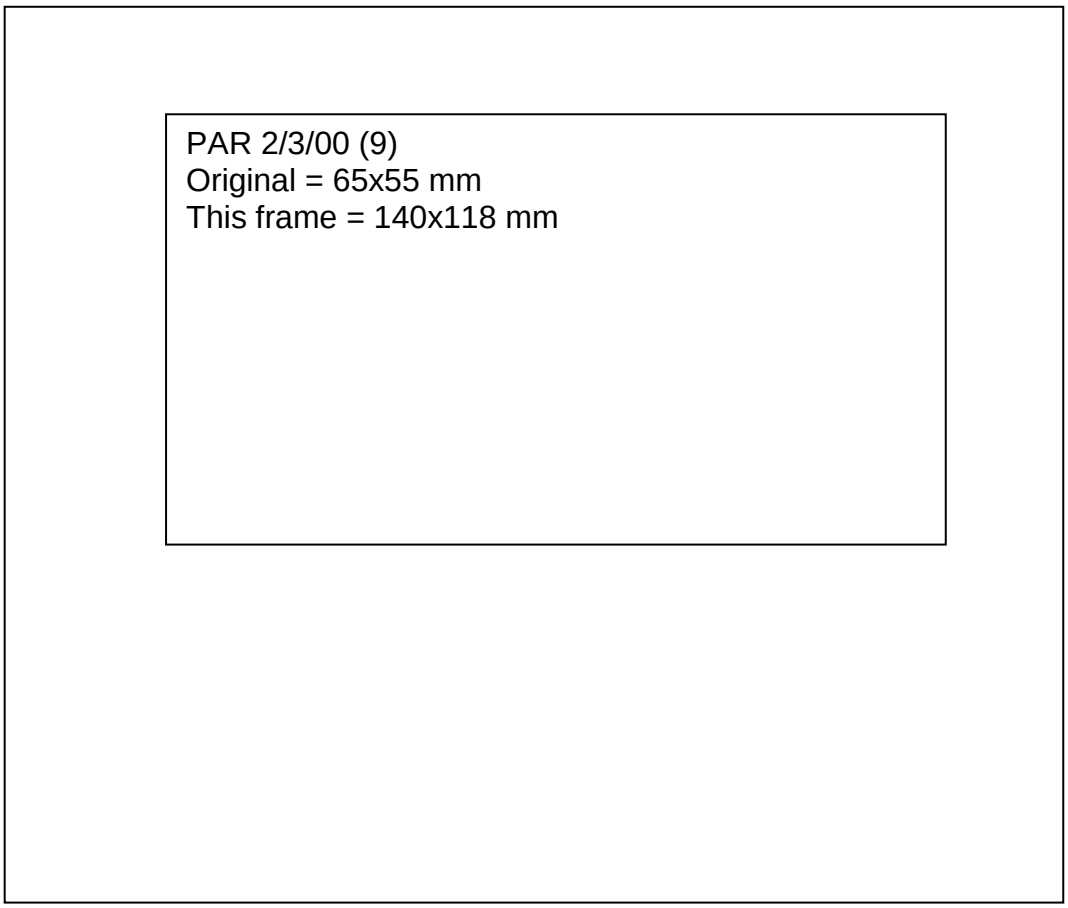

Three long structures of different lengths can be seen on this micrograph of *S. gordonii* PAR. Shorter fibrils are also visible (arrow).

***S. gordonii* MJ2.** Long structures were present in low levels on the surface of *S. gordonii* MJ2, which was dominated by many fibrils, as shown in Figure 11.

Figure 11. Electron micrograph of *S. gordonii* MJ2

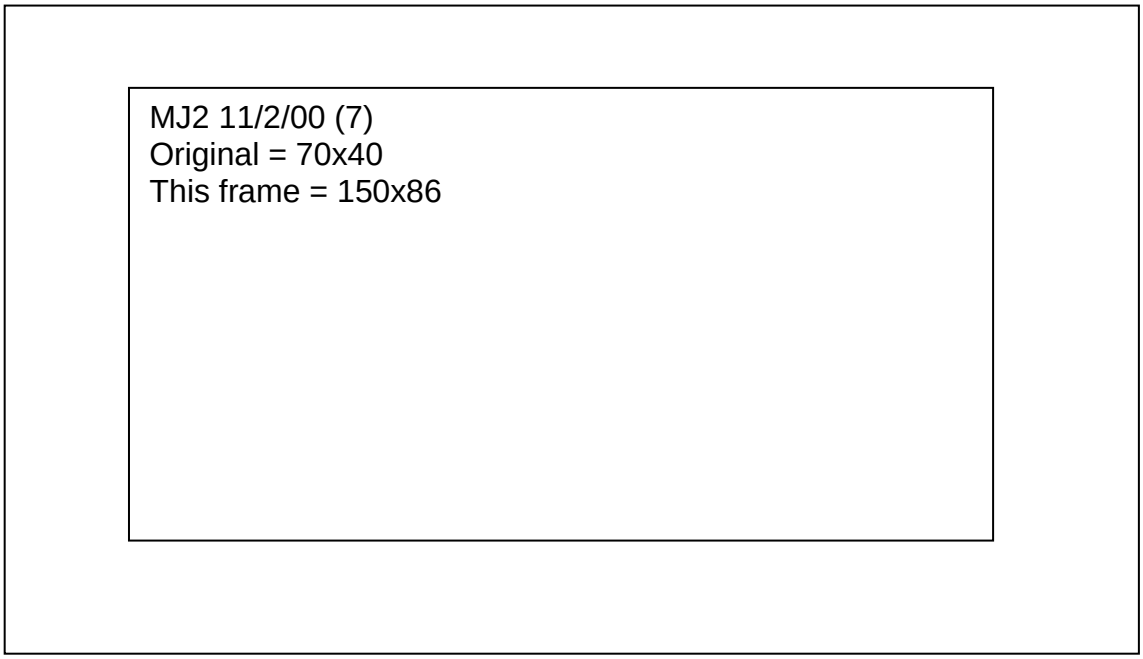

The surface of *S. gordonii* MJ2 is dominated by short fibrils

***S. oralis* NCTC 11427, *S. oralis* EY3 and *S. oralis* 34.** Sparse short fibrils were observed on the surface of *S. oralis* EY3. Examination of *S. oralis* 34 revealed the presence of short fibrils and longer structures (not shown). *S. oralis* NCTC 11427 was not examined, and its surface structure remains unknown.

Analysis of fibril length and gold distance measurements taken from electron micrographs

In order to highlight the predominant fibril lengths and gold distances measured, the measurements were ranked and plotted as a line graph to reveal the profile of the data (Figure 12). This form of fibril length analysis typically produced a long straight line with a shallow gradient, representing the majority of the data points. Upon reaching a certain fibril length, the frequency of measurements usually reduced, causing an increase in the gradient of the line. Interpretation of line graphs such as those shown in Figure 12, is

difficult, so line graphs are presented for one strain only (*S. sanguis* FC1) for illustration purposes. The same data can be more easily interpreted when shown as a histogram. Histograms are used to present the measurements taken from all strains (Figures 13 - 16), showing the frequency of measurements taken within defined 10 nm ranges so that the predominant range can be clearly seen.

The majority of measurements, and the most frequent measurements for fibrils and gold on all strains were between 0 and 150 nm, therefore this range is used to present the data from most sets of measurements, even though there were usually measurements taken beyond this range. The low frequency of fibril length measurements of structures over 150 nm, and the decreased probability of longer structures being normal to the cell make these measurements statistically unreliable, however, they are mentioned in the text.

Fibril Length Analysis

The greatest number of fibril measurements were taken from *S. sanguis* FC1 (Figures 12a, 13a) and *S. gordonii* PAR (Figure 14a) (around 50 cells used for each set of measurements). For both of these organisms the most frequent fibril length measured was between 50 and 80 nm with a sharp drop in measurements either side of this range. There is a second, smaller peak of measurements between 120 and 150 nm for *S. gordonii* PAR (Figure 14a), and a possible similar secondary peak (five measurements) between 150 and 170 nm from the surface of *S. sanguis* FC1 (Figure 13a). Fibril measurements made on *S. gordonii* MJ2 produced a single clear frequency peak at fibril lengths between 40 and 60 nm (Figure 16a).

Fewer pictures were used to obtain measurements from *S. sanguis* NCTC 10904 and no clear peak emerged, though the highest frequency of fibril measurements were again taken from the range of 50 – 80 nm (Figure 15a). Due to preparation difficulties, the electron micrographs of *S. oralis* EY3 were of too low quality to obtain sufficient measurements for confident interpretation. The low frequency of fibril measurements below 30 nm is due

to the decision not to measure fibrils appearing significantly shorter than the fringe or other fibrils.

To obtain a figure for mean fibril lengths and gold distance measurements, the peak representing the measurements was identified on the histogram. The measurements making up the peak (which may span more than one 10 nm range), and the 10 nm measurement ranges adjacent to the peak were selected to obtain a mean. A mean value was determined for each fibril class and gold distance peak identified, summarised in Table 3.

Table 3. Summary of fibril lengths and gold distance measurements

Strain	Fibril length		Gold distance	
	Mean length (nm)	**Standard deviation (n)**	**Mean distance (nm)**	**Standard deviation (n)**
S. sanguis FC1	<u>67.3</u>	11.4 (35)	<u>23.1</u>	9.1 (110)
	160.2	7.0 (5)	52.1	13.1 (121)
			131.1	13.9 (28)
S. sanguis NCTC 10904	<u>65.9</u>	12.3 (10)	21.7	9.9 (35)
	161	2.5 (3)	<u>48.7</u>	10.8 (41)
			131.3	8.8 (10)
			177.5**	8.1 (8)
S. gordonii PAR	<u>63.6</u>	11.9 (19)	<u>55.5</u>	7.3 (39)
	133.4	11.7 (7)	116.0	13.1 (36)
S. gordonii MJ2 *	<u>50.6</u>	9.4 (41)	<u>25.5</u>	7.2 (51)
			132.8	7.3 (7)
All strains	<u>59.7</u>	14.3 (114)	<u>22.8</u>	9.2 (229)
			49.3	10.9 (219)
			128.7	10.0 (68)

Mean fibril lengths and gold distances were determined from the measurements making up peaks on histograms (figures 11 - 14). In most cases more than a single peak was identified, indicating the presence of fibrils of different lengths and preferential gold binding at various distances from the cell. The largest peak for each category is underlined. Standard deviations are shown with the number of measurements used to determine the mean and standard deviation in brackets.

*** Separate broths used for fibril measurement and gold distance measurement**

**** Peak not shown on histogram**

Gold Distance from Cell Surface

The most frequent distance at which gold particles were measured from the surface of *S. sanguis* FC1 was 10-20 nm, with a gradual decline in frequency moving out from the cell (Figure 12b, 13b). This general decline is interrupted by an increase to a peak between 50 and 60 nm from the cell surface (peak represents a 31 % increase in frequency compared to measurements taken from adjacent 10 nm ranges). The lowest measurement frequency was obtained between 100 and 110 nm from the surface, and levels remained low beyond this distance. The gold particles used to label *S. gordonii* PAR were detected at relatively constant frequency in the range of 10 – 150 nm from the cell surface, except for a prominent peak of measurements between 50 and 60 nm (Figure 14b). The resolution of the data from gold distance measurements on *S. sanguis* NCTC 10904 (Figure 15b) is lower than that for *S. sanguis* FC1 and *S. gordonii* PAR because of the smaller number of measurements. However, there is clearly a greater frequency of measurements in the range of 0 – 60 nm, compared to 60 – 150 nm from the cell surface, and the particles were most frequently found between 40 and 60 nm from the cell surface. The most frequent distance of gold particles from the cell surface of *S. gordonii* MJ2 was between 20 and 30 nm, and a low frequency of particles were counted beyond 50 nm from the surface (Figure 16b).

Correlation between Fibril Length and Gold Distance Measurements, and similarities between strains

The most frequent 10 nm measurement range for fibrils and gold distances correspond exactly (50 – 60 nm) for *S. gordonii* PAR (Figure 14a, 14b) and *S. sanguis* FC1 (Figure 13a, 13b), however the *S. sanguis* FC1 gold distance peak is a secondary peak. The profile of fibril measurements taken from these two organisms are also remarkably similar, having a low frequency up to 50 nm, a maximum between 50 and 60 nm, a secondary maximum between 70 and 80 nm, and a low frequency of measurements above 80 nm.

There are not enough fibril measurements to allow the interpretation of two separate fibril peaks for these strains to be made with any certainty; it is more likely that the data represents a single peak for each strain in the range of 50 - 80 nm.

The mean fibril lengths of *S.sanguis* FC1, *S. sanguis* NCTC 10904, and *S. gordonii* PAR were 67.3 nm, 65.9 nm and 63.6 nm respectively, spanning a range of less than 5 nm (Table 3). The mean of gold distance peaks for these strains most closely matching the fibril peaks were 52.1 nm, 48.7 nm and 55.5 nm respectively, averaging 13.5 nm closer to the cell surface than the fibril tip (Table 3). Though only supported by relatively few measurements, the mean length of longer structures was also determined for these three strains; for both strains of *S. sanguis* a mean length of approximately 160 nm was found, and for *S. gordonii* PAR the mean length was 133 nm. Further mean peak gold distance measurements are listed in table 3.

Only one fibril length peak is evident in the *S. gordonii* MJ2 histogram, revealing a mean fibril length of 50.6 nm, approximately 15 nm shorter than the fibrils shown for the other three strains in Table 3. The peak distances of gold particles from the surface of *S. gordonii* MJ2 cells had means of 25.5 nm and 132.2 nm. The shortest peak gold distance from the surface of *S. gordonii* MJ2 is approximately 25 nm closer to the cell than the peak distance of fibril tips from the surface (51 nm) (Figure 16a, 16b). Fibril and gold distance measurements made on *S. gordonii* MJ2 used cells from separate broths, so the relationship between gold distance and fibril length is not protected against batch to batch variation.

The fibril length peak for *S. sanguis* NCTC 10904 is between 60 and 70 nm, but is made of too few measurements to be relied upon (Figure 15a). The peak of gold distance measurements for this strain occurs between 40 and 60 nm from the cell surface (Figure 15b), coinciding with the gold distance peaks of *S. gordonii* PAR and *S. sanguis* FC1.

Figure 12. Line graphs of ranked fibril lengths and gold distance measurements for *S. sanguis* FC1

a.

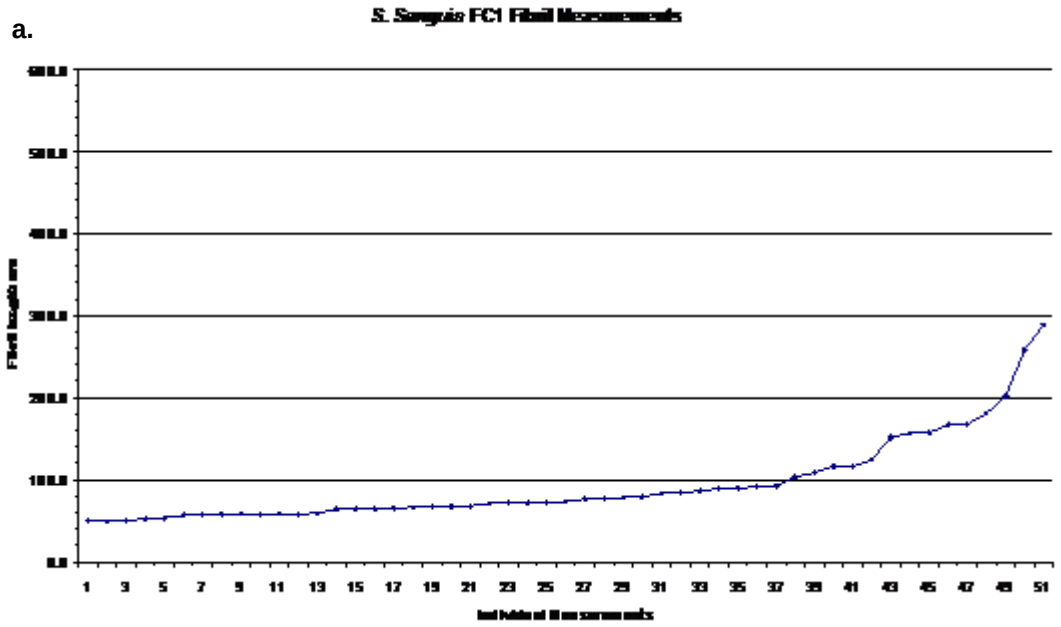

b.

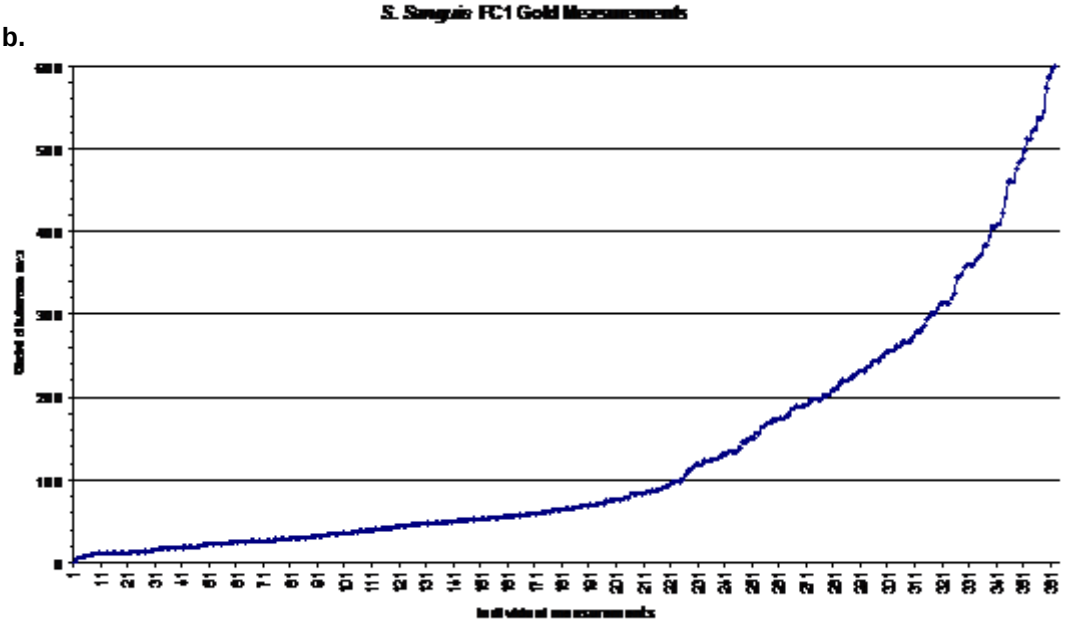

a. individual fibril length measurements made from electron micrographs of negatively stained cells

b. individual gold distance measurements made from electron micrographs of negatively stained immuno-gold labelled cells

Figure 13. Histograms representing measurements of fibril length and gold distance from *S. sanguis* FC1

a.

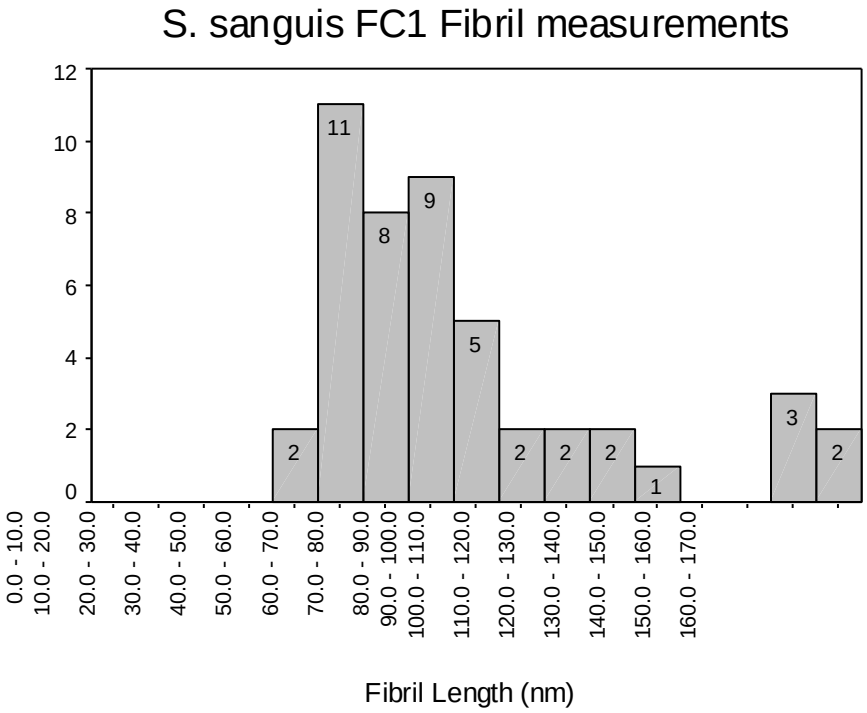

b.

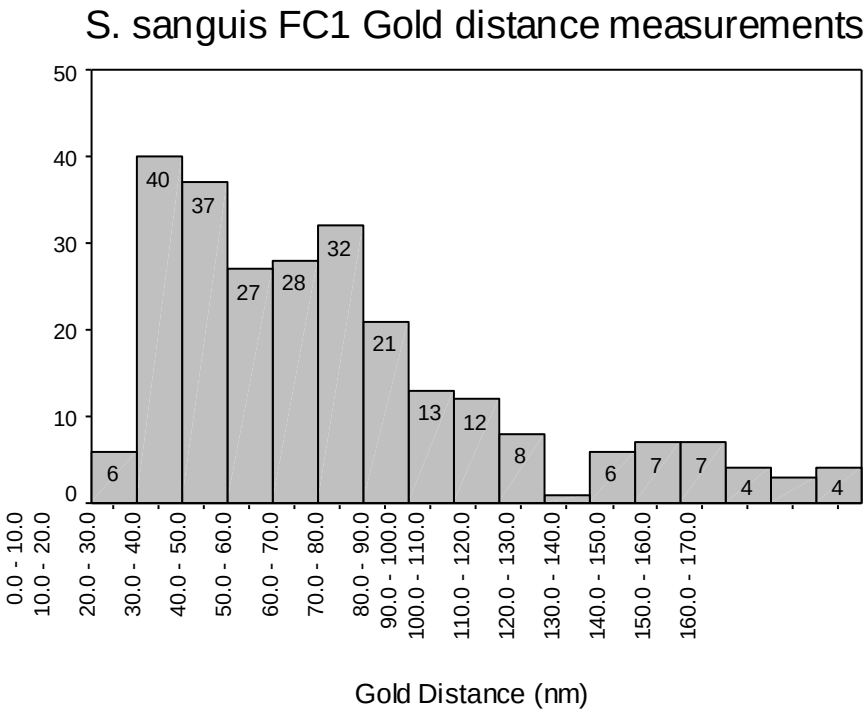

Histograms showing the profile of fibril length (a), and gold distance from cell surface (b) measurements made on electron micrographs of *S. sanguis* FC1. The histograms represent the same data as figure 10, showing the frequency of measurements for particular measurement ranges.

Figure 14. Histograms representing measurements of fibril length and gold distance from *S. gordonii* PAR

a.

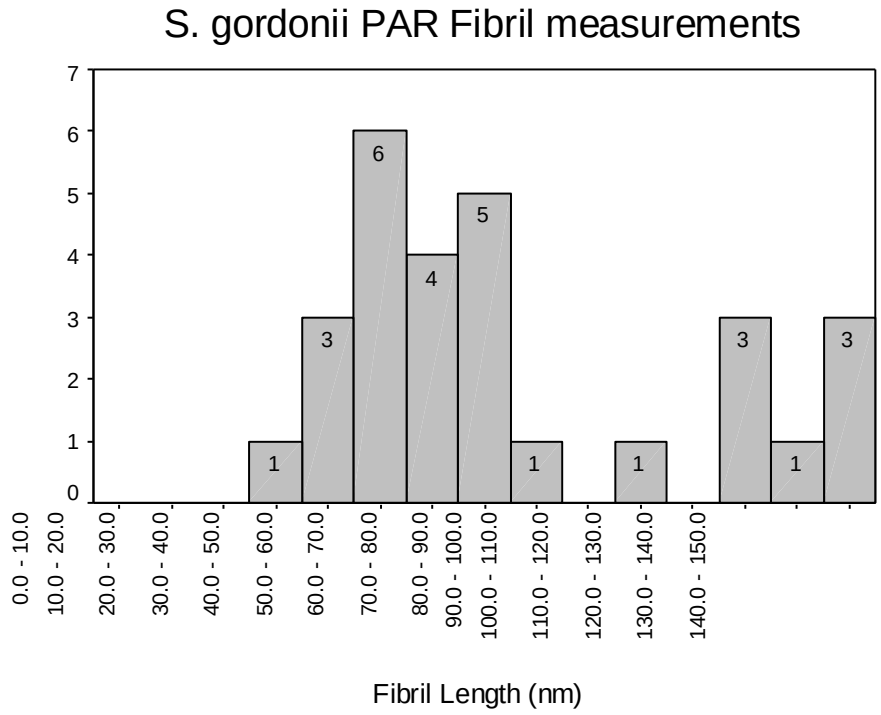

b.

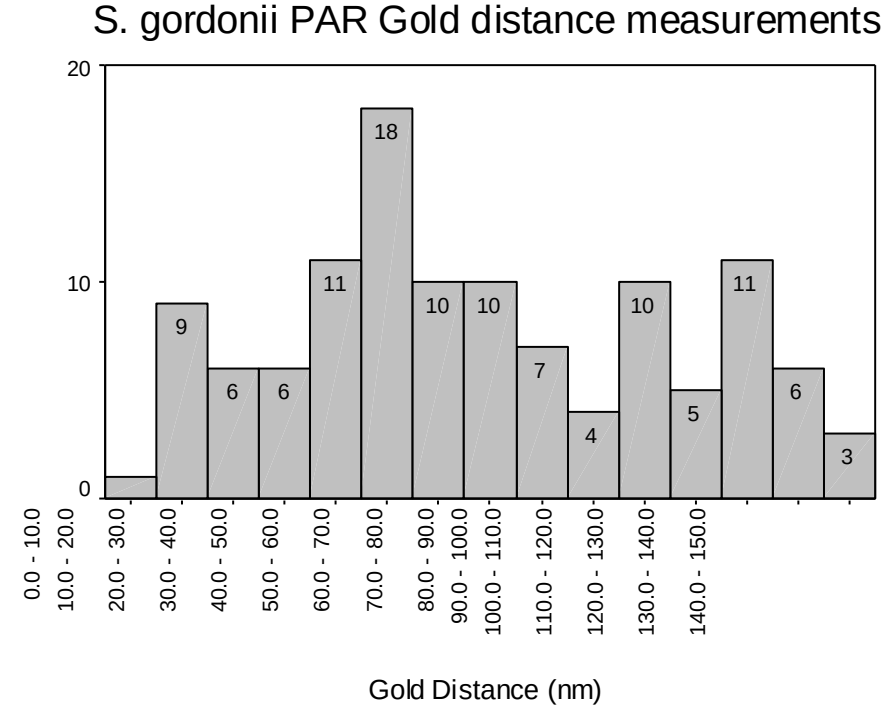

Histograms showing the profile of fibril length (a), and gold distance from cell surface (b) measurements made on electron micrographs of *S. gordonii* PAR.

Figure 15. Histograms representing measurements of fibril length and gold distance from *S. sanquis* NCTC 10904

a.

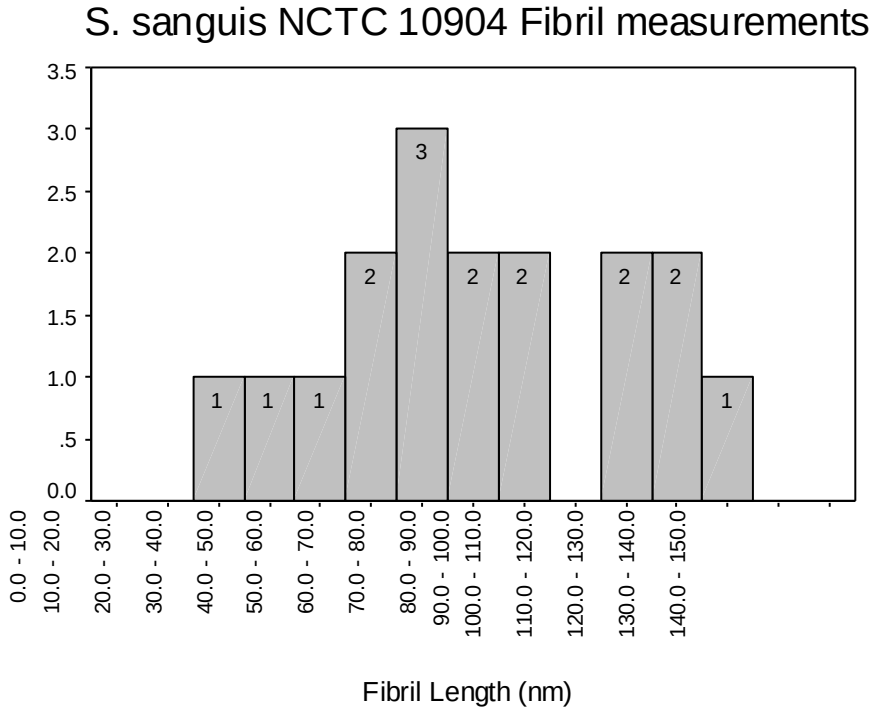

b.

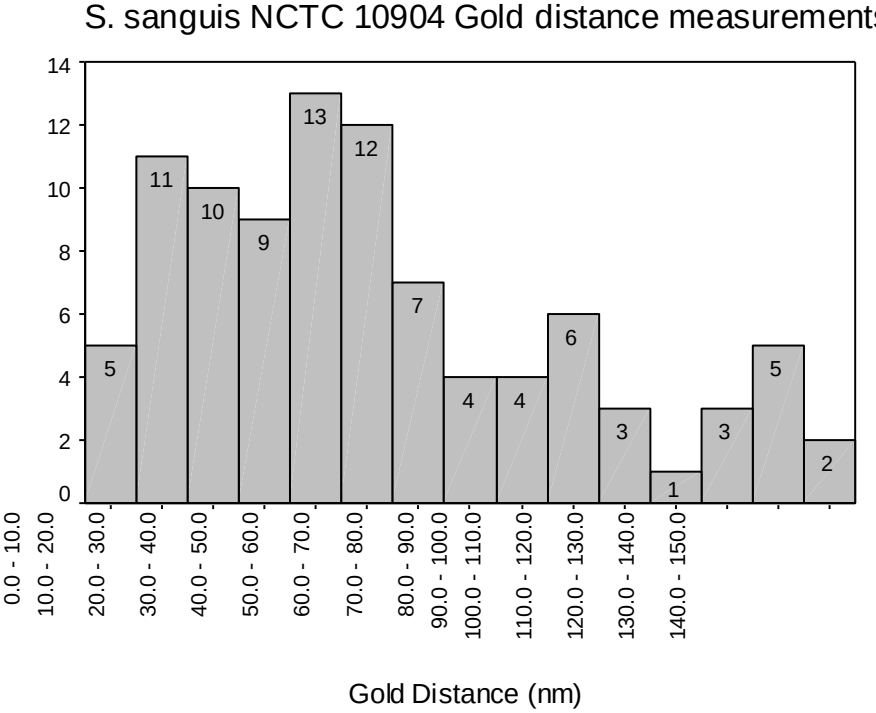

Histograms showing the profile of fibril length (a), and gold distance from cell surface (b) measurements made on electron micrographs of *S. sanguis* NCTC 10904.

Figure 16. Histograms representing measurements of fibril length and gold distance from *S. gordonii* MJ2

a.

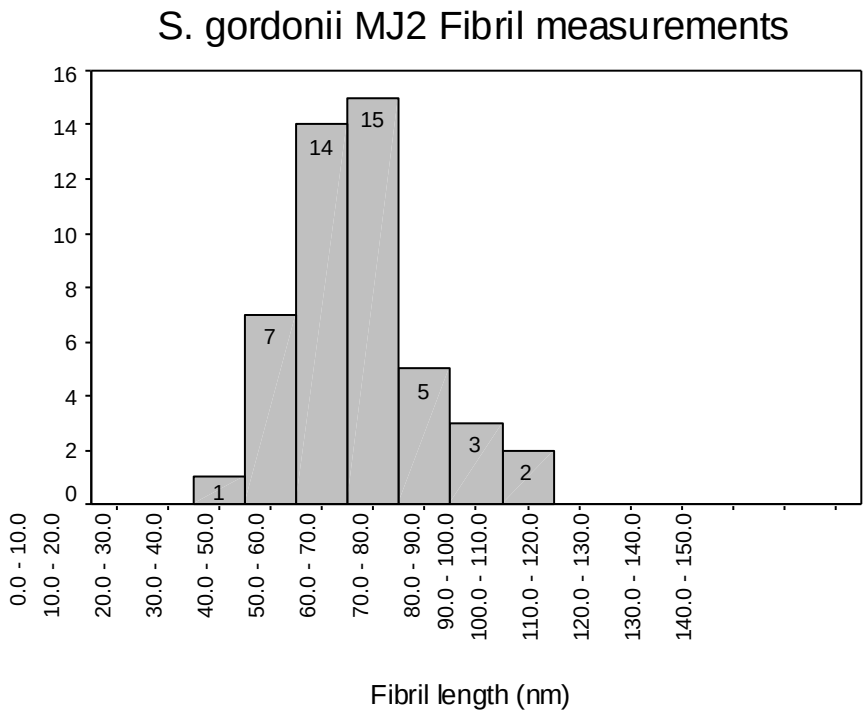

b.

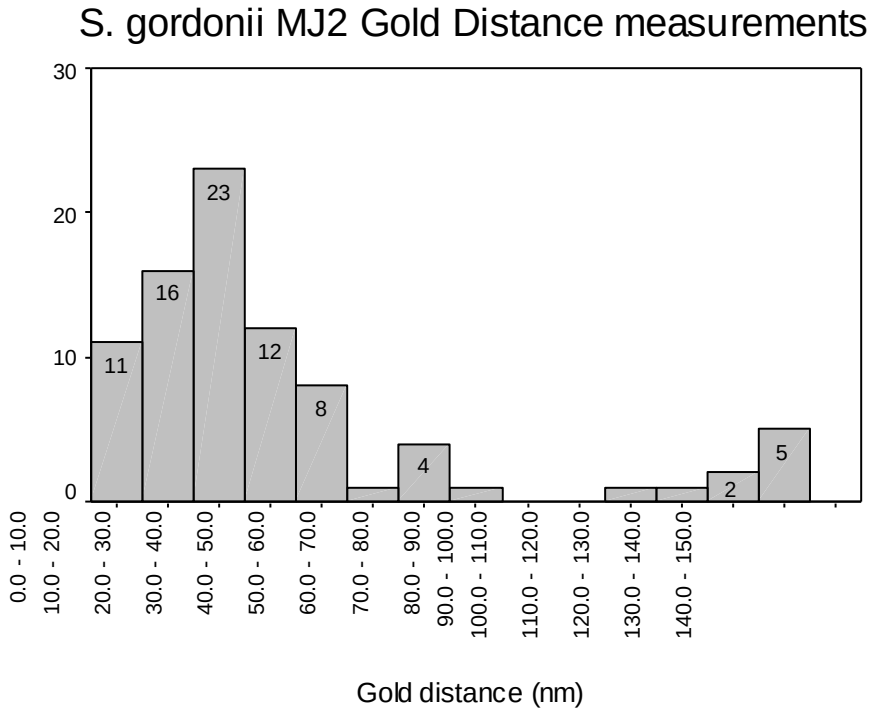

Histograms showing the profile of fibril length (a), and gold distance from cell surface (b) measurements made on electron micrographs of *S gordonii* MJ2. Separate broths were used to provide cells for fibril measurements and gold distance measurements.

To highlight any fibril length or gold distance trends, which are common to all of the strains measured, the data has been combined and presented in figure 17 as histograms. From figure 17 it can be seen that there is a single large peak of fibril measurements centred between fibril lengths of 50 and 60 nm. There is no other obvious peak of fibrils, but there is a low level of structures measured between 80 and 170 nm, and a very low frequency of measurements made over 170 nm long. The combined gold distance measurements also have a peak between 50 and 60 nm, but a slightly higher frequency of gold particles were measured between 10 and 30 nm from the cell surface. The frequency of gold particles measured at over 100 nm from the cell surface is low, except for a slight peak between 120 and 140 nm.

Figure 17. Histograms representing combined measurements of fibril length and gold distance

a.

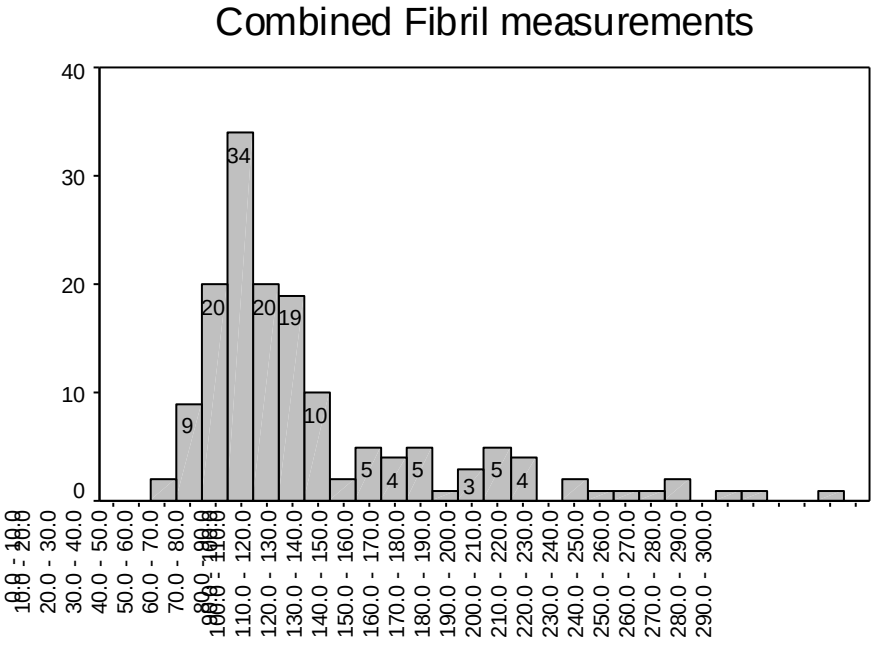

b.

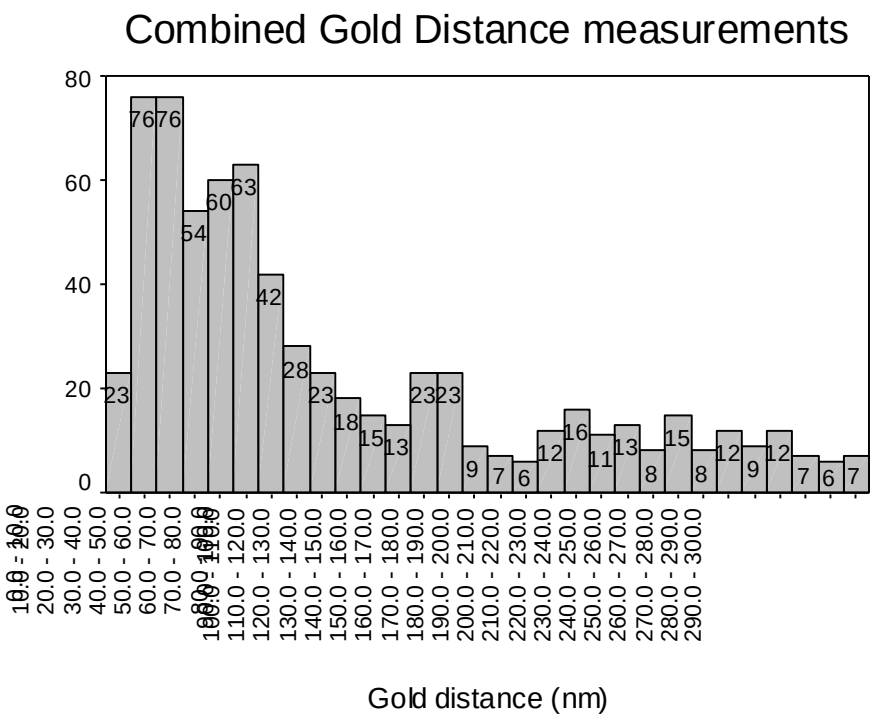

Histograms showing the profile of fibril length (a), and gold distance from cell surface (b) measurements made on electron micrographs of *S. gordonii* PAR, *S. gordonii* MJ2, *S. sanguis* FC1 and *S. sanguis* NCTC 10904.

DISCUSSION

Detection of CshA N-terminal region on oral streptococci by ELISA

Distinct groups of strains could be defined based upon the level of ELISA reaction observed. This may be a result of assaying a relatively small number of strains, or it could represent the existence of a number of distinct modes (e.g. peritrichous or tufted fibrils) of cell surface CshA expression.

The low reactivity group included the $CshA^-$, $CshB^-$ mutant of *S. gordonii* DL1 - *S. gordonii* OB277, and the non-hydrophobic, bald mutant of *S. sanguis* FC1 - *S. sanguis* nhm. The wild type parents of these mutants were in the high and medium reactivity groups respectively, indicating that a loss of surface structures, in particular the loss of CshA and CshB polypeptides from the cell surface, results in the complete loss of anti-N-CshA antiserum reactivity in this assay. The other eight streptococcal strains, which are in the low reactivity group, represent approximately half of the wild type strains tested and are thought not to express CshA on their surface. Some of these strains produced a weak positive ELISA reaction, but when compared to the positive results of the medium and high reactivity strains it is considered likely that these reactions represent noise in the assay caused by non-specific binding etc. It is possible however, that these reactions represent very low levels of cell-surface exposed CshA, or higher levels of antigenic variants of CshA. The highest reactivity was, not surprisingly produced by *S. gordonii* DL1, already known to express CshA as fibrils and the source of the N-CshA antigen used to raise the antiserum for this assay. The density of cell surface fibrils does not correlate with the level of CshA detected by the ELISA (Table 1, 2), suggesting that the fibrils on some strains at least, are not composed of CshA.

The ELISA allowed a selection of oral streptococci to be quickly screened to identify strains expressing CshA on the cell surface. Strains positively identified as expressing CshA included members of *S. sanguis*, *S. oralis*, and *S. gordonii*, clearly showing that CshA is not confined to *S. gordonii*. Only

38 % of *wild type S. gordonii* strains tested gave a result clearly indicating surface expression of CshA, suggesting that the CshA polypeptide is not universally present among this group. One of the wild type *S. sanguis* strains, and the single *S. mitis* and *S. crista* strains tested also did not appear to express CshA. The failure of a particular strain to produce a definite positive ELISA reaction does not necessarily mean that CshA-like polypeptides are absent from that strain. It is possible that the N-terminal primary antiserum failed to recognise CshA-like polypeptides which differed antigenically from the *S. gordonii* DL1 CshA polypeptide in their N-terminal region. The N-terminal portion of CshA is thought to contain the specific adhesion-mediating domain (McNab *et al* 1996), and it is possible that variations in this region exist to confer different adhesive properties. Another possibility is that CshA expression is regulated so that certain strains capable of CshA expression did not produce the polypeptide because of the experimental conditions employed. However, this is considered unlikely given the wide range of conditions likely to be experienced during batch growth, and the finding of McNab and Jenkinson (1998) that the promoter of the *S. gordonii* DL1 *cshA* gene is most active in late exponential phase. The possibility of N-terminal variations in CshA causing low reactions could be investigated by repeating the ELISA using a C-terminal or whole molecule anti-CshA primary antiserum.

The absorbance results obtained are assumed to represent the abundance of cell surface exposed polypeptides, which are specifically bound by the N-CshA primary antiserum. Many other factors may have had an influence on the results, possibly contributing to the formation of different reactivity groups. Different configurations of CshA on the cell surface, such as tufts of fibrils or peritrichous fibrils, steric hindrance by other surface structures, co-aggregation of bacteria and different levels of binding to the microtitre plates between strains may all potentially have an effect on the ELISA result.

Analysis of Cell Surface Structures and N-CshA antiserum binding by Electron Microscopy

All of the strains from the high N-CshA ELISA reactivity group were negatively stained and viewed in the electron microscope, except for *S. gordonii* DL1 which has already been extensively studied (McNab *et al* 1999). Negative staining revealed at least two distinct classes of surface structure defined by length, simultaneously present on all of these strains. Long structures were typically between 130 and 160 nm long, and fibrils were approximately 65 nm in length, similar to the 60.7 nm long CshA fibrils of *S. gordonii* DL1 measured by McNab *et al* (1999). The longer structures were often difficult to measure due to bending and tangling with each other; however, these structures sometimes radiated straight out from the cell, allowing measurements to be made. Measurements from long structures indicate that their length is not fixed, but variable, suggesting that they are in continuous growth, and perhaps also subject to shrinkage. The most likely explanation for this finding is that the long structures have a subunit structure like the fimbriae described for many Gram negative bacteria. The shorter structures are described as fibrils and clearly have a fixed length, suggesting a non-repeating structure, such as a single polypeptide. *S. sanguis* nhm, a non-hydrophobic mutant of *S. sanguis* FC1, produced a low reactivity with the N-CshA ELISA, and negative staining confirmed the mutant to lack the surface structures described above for the highly reactive strains (including its parent). This is in agreement with Gibbons *et al* (1983), who originally isolated the mutant and reported it to lack fimbriae. The correlation between loss of surface structures and loss of reactivity with anti-N-CshA antiserum supports the findings of McNab *et al* (1999), who showed that CshA is the structural and functional component of *S. gordonii* fibrils.

Immuno-gold labelling was performed on the same strains that were negatively stained, with the exception of *S. oralis* 34, which was omitted due to time constraints. The vast majority of fibrils and other surface structures were obscured by the gold labelling process, preventing a direct visual identification of the location of CshA on the cell surface. It could be seen that the majority of gold particles in association with the cell were not bound

directly to the cell wall, but were held close to the cell, suggesting an association with the fibrils or other hair like surface structures previously observed. The shortest class of fibrils measured on *S. sanguis* FC1, *S. sanguis* NCTC 10904, and *S. gordonii* PAR were all found to have a mean length between 63 and 68 nm; the difference in length between these fibrils is considered to be insignificant and the fibrils were indistinguishable from each other on electron micrographs. In addition, the gold labelling patterns of these strains were similar, and all revealed a peak of anti-N-CshA binding approximately 52 nm from the cell surface, indicating that the N-terminal regions of CshA polypeptides are concentrated at this distance (among others, discussed later) from the cell surface.

These results support the hypothesis that the CshA polypeptide is the structural protein observed as fibrils in negatively stained preparations of *S. gordonii* PAR, *S. sanguis* NCTC 10904, and *S. sanguis* FC1. In addition, the CshA fibrils of these strains appear to be identical, with the CshA polypeptide anchored in the cell wall at it's C-terminus, and the N-terminal region distal to the cell. In support of this hypothesis, the detection of gold particles approximately 14 nm closer to the cell surface than the fibril tips can be explained by a number of possibilities, summarised in Figure 15. The anti-N-CshA may firstly be binding to a part of the 844 amino acid fragment used to generate the antiserum, which is not expressed at the fibril tip, but closer to the cell. Alternatively, the multivalent goat-anti-rabbit gold conjugate may cause a number of fibril tips coated in rabbit anti-N-CshA, to become simultaneously bound to a single gold particle, thus drawing it closer to the cell. This effect has been observed on a number of electron micrographs, and is typically seen as a triangular structure made between the cell wall and two or more distinct fibrils with a gold particle at the apex (Figure 8, 18). Another obvious possibility is that fibrils are not always normal to the cell surface, but fall or bend over; an effect which may be increased on fibrils burdened with an attached gold particle. A final possibility is that the fibril may undergo a conformational change upon binding, causing the length of the fibril to reduce.

Figure 15. Factors potentially influencing gold distance measurements from the cell surface of cells that have been immuno gold labelled to reveal the position of the CshA polypeptide N-terminal region

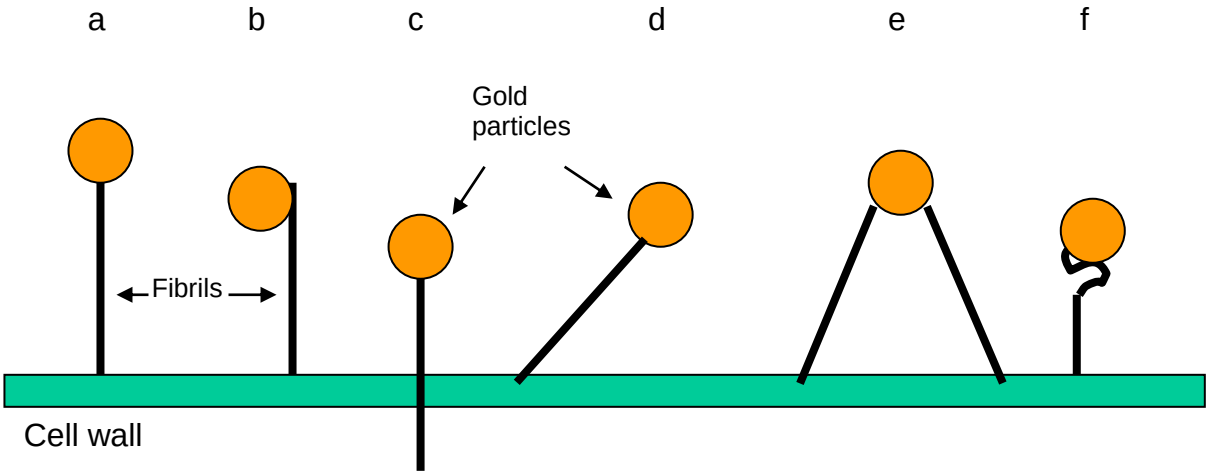

The orientation of fibrils, the position at which anti-N-CshA antiserum binds to fibrils, and conformational changes in fibrils may all affect the distance at which gold particles are bound from the cell surface after immuno-gold labelling.

a. Fibril with gold particle bound at tip

b. Fibril with gold particle bound to side of tip

c. Fibril at partial extension with gold particle bound at fibril tip

d. Fallen fibril with gold particle bound to tip

e. Two or more fibrils binding a single gold particle, drawing it closer to the cell

f. Conformational change induced by binding to fibril

The peaks of gold particles above proposed to be adhering to the N-terminal region of fibrillar CshA polypeptide, represent the most prominent gold distance measurements made from *S. gordonii* PAR and *S. sanguis* NCTC 10904, and the second most prominent distance measured for *S. sanguis* FC1. The greatest gold distance peak of *S. sanguis* FC1, and lesser peaks of *S. sanguis* NCTC 10904 and *S. gordonii* PAR occurred at approximately 20 nm distance from the cell surface. A peak of gold binding close to the cell surface is not expected with the hypothesis that the N-terminus of the CshA polypeptide forms fibril tips distal to the cell, however it may be explained by a number of possibilities, the most likely of which is that fallen fibrils are lying on the cell surface. There is generally a high incidence of gold particles found all the way from the cell surface, up to the maximum fibril extension, beyond which there is a drop in the frequency of gold particles (*S. gordonii* PAR is an

exception). This supports the idea that fibrils composed of CshA extend through the cell wall to a maximum length, and that gold-labelled fibrils may fall over and stick together, possibly resulting in a high incidence of gold particles close to the cell surface. Another explanation for the high incidence of gold labelling close to the cell surface and within the fibrillar fringe, is that the fibrils are bound by anti-N-CshA antiserum throughout their length, and not specifically at the tip. The implication of this is that the fibrils are composed of many individual CshA polypeptides, which present their N-terminal region along the length of the fibril. This is considered unlikely because the small number of electron micrographs showing gold particles attached to visible fibrils, indicate that the anti-N-CshA antiserum binds to the fibril tip. In addition, CshA fibrils are probably composed of only a single polypeptide, since *cshA* gene disruption or heterologous insertion is sufficient to prevent or induce fibril expression (McNab *et al* 1999), and it is difficult to see how a multimeric arrangement of a single polypeptide could produce fibrils of consistent length.

Apart from *S. gordonii* DL1 (whose *cshA* gene was cloned and expressed to produce anti-N-CshA antiserum), the highest ELISA result obtained for reactivity with anti-N-CshA was for *S. gordonii* MJ2. The only mean fibril length obtained for this strain was 50.6 nm, 10 – 20 nm shorter than the fibril length determined from the three strains described above, and the only substantial peak of gold particles occurred at a distance of 25.5 nm from the cell surface. Given the consistent fibril lengths and gold distance measurements taken from the other three strains, it is considered most likely that the different fibril and gold distance profile observed for *S. gordonii* MJ2 represents a genuine difference in this strain compared to the other three. However, this difference is not believed to be the result of *S. gordonii* MJ2 having shorter fibrils, but rather a consequence of the high density of CshA fibrils on the cell surface. The ELISA showed a high incidence of CshA on the surface of this strain, and electron micrographs revealed a high density of fibrils, which may result in the clumping and contraction of fibrils, especially after gold labelling. A high rate of fibril production may also result in an increased proportion of incompletely extended fibrils on the cell surface. It is

possible that the CshA gene of *S. gordonii* MJ2 has fewer repeat blocks, or differs in other ways from the genes of the other strains, resulting in the production of shorter fibrils.

For all strains, the number of long structures measured was lower than the number of fibrils, and the corresponding measurements of gold distance from the cell surface were also less frequent. The apparent low frequency of long structures on cell surfaces may be misleading, as many cell surfaces appeared to be dominated with longer structures, having a lower frequency of shorter fibrils, but the difficulty of measuring long structures led to many not being measured. No clear peaks in gold distance frequency were observed to correspond with the long structure measurements, and it is believed from this result that the anti-N-CshA antiserum did not bind these long structures. It is possible however, that the antiserum did bind to these structures, but they may have fallen towards the cell surface or become stuck together as proposed for fibrils, obscuring any peak in gold binding distance. This effect would be greater for long structures compared to fibrils. However, if gold particles selectively bind to longer structures then there would be a relatively high level of gold particles within the range of the long structures (<170 nm), followed by a drop beyond the distance at which gold particles can be bound. Such a pattern was not observed.

CshA fibrils have previously been reported to have a globular tip (McNab *et al* 1999), similar to that of purified *S. salivarius* fibrillar proteins (Weerkamp *et al* 1986). Observations from negatively stained cells, coupled with the interpretation of fibrils on these cells being composed of CshA, suggests that CshA fibrils do not have a globular tip. The vast majority of fibrils seen throughout this study did not have globular tips, but a small number of fibrils with globular tips were seen. The most likely explanation for this, and previous reports of CshA fibrils having a globular tip, is considered to be that the CshA fibril tip appears globular when bound to certain molecules which may be present in the medium. It is also possible that the fibrils with globular tips represent a separate fibril class, or the same fibrils in a different structural conformation.

CONCLUSIONS

A new approach to the measurement and characterisation of hair-like surface structures has been developed and used to obtain accurate measurements of streptococcal fibrils. Fibrils may appear shorter than their true length in electron micrographs for various reasons, including being anchored deep within the cell wall or behind the edge viewed on the micrograph. Longer structures observed on electron micrographs were typically 160 nm in length, and are not thought to contain the CshA polypeptide, due to the failure to detect any binding of anti-N-CshA antiserum to these structures. These longer structures may be similar to the fimbriae of Gram negative organisms, composed of protein subunits. Experimentation with buffers and washing procedures may help bacterial surface structures to remain extended to facilitate measurement, which was difficult for some of the longer structures seen in this study.

The CshA polypeptide is widely distributed among the oral streptococci investigated, and for the first time has been found to be present as fibrils on the cell surfaces of strains of *S. gordonii*, *S. sanguis* and *S. oralis*, though it is not necessarily present on all members belonging to these groups. CshA is expressed on the surface of streptococci to form fibrils approximately 60 nm in length, with the N-terminal region of the polypeptide distal from the cell. These fibrils are found in greatest number on regions of old cell wall, and do not appear to have a globular tip, except for on a small minority of fibrils, which may appear globular as a result of binding to components in the medium. The finding that CshA is widespread on the surfaces of oral streptococci, in combination with the fact that CshA and CshB are required for colonisation of the oral cavity by *S. gordonii* (McNab *et al* 1994), provides further evidence that CshA may be an important factor in the colonisation of the oral cavity by streptococci. Whether CshA has a specific adhesive role in the mouth, or is a general streptococcal adhesin could be investigated by performing an ELISA to detect CshA on the surfaces of streptococci isolated from other sites, both medical and environmental.

REFERENCES

Gibbons RJ, Etherdon I, Skobe Z (1983). Association of Fimbriae with Hydrophobicity of *Streptococcus sanguis* FC-1 and Adherence to Salivary Pellicles. *Infection and Immunity* **41(1):** 414-417

Handley PS, Carter PL, Wyatt JE and Hesketh LM (1985). Surface Structures (Peritrichous Fibrils and Tufts of Fibrils) Found on *Streptococcus sanguis* Strains May be Related to Their Ability to Coaggregate with Other Oral Genera. *Infection and Immunity* **47(1):** 217-227

Handley PS, McNab R and Jenkinson HF (1999). Adhesive Surface Structures on Oral Bacteria. *Eastman Dental Conference* 1999.

Holmes AR, Gopal PK and Jenkinson HF (1995). Adherence of *Candida albicans* to a cell surface polysaccharide receptor on *Streptococcus gordonii*. *Infection and Immunity* **63:** 1827-1834

Marsh PD and Martin MV (1999). Chapter 1 in "*Oral Microbiology, fourth Ed.*" Pub: Wright, Oxford. pp 1-4

McNab R, Jenkinson HF, Loach DM, and Tannock GW (1994). Cell-surface associated polypeptides CshA and CshB of high molecular mass are colonization determinants in the oral bacterium *Streptococcus gordonii*. *Molecular Microbiology* **14(4):** 743-754

McNab R, Holmes AR, Clarke JM, Tannock GW and Jenkinson HF (1996). Cell surface polypeptide CshA mediates binding of *Streptococcus gordonii* to other oral bacteria and to immobilized fibronectin. *Infection and Immunity* **64:** 4204-4210

McNab R and Jenkinson HF (1998). Altered adherence properties of a *Streptococcus gordonii hppA* (oligopeptide permease) mutant result from

transcriptional effects on *cshA* adhesin gene expression. *Microbiology* **144:** 127-136

McNab R, Forbes HF, Handley PS, Loach DM, Tannock GW and Jenkinson HF (1999). Cell Wall-Anchored CshA Polypeptide (259 Kilodaltons) in *Streptococcus gordonii* Forms Surface Fibrils That Confer Hydrophobic and Adhesive Properties. *Journal of Bacteriology* **181(10):** 3087-3095

Niedhardt FC, Ingraham JL, and Schaechter M (1990). Assembly and Polymerization: The Bacterial Envelope, *In, Physiology of the Bacterial Cell: A Molecular Approach*. Pub: Sinaver Associates, Inc., Massachusettes. pp 102-132

Soto GE and Hultgren SJ (1999). Bacterial Adhesins: Common Themes and Variations in Architecture and Assembly. *Journal of Bacteriology* **181(4):** 1059-1071

Weerkamp AH, van der Mei HC, and Liem RSB (1986). Structural properties of fibrillar proteins isolated from the cell surface and cytoplasm of *Streptococcus salivarius* (K^+) cells and nonadhesive mutants. *Journal of Bacteriology* **165:** 756-762

Whittaker CJ, Klier CM, and Kolenbrander PE (1996). Mechanisms of Adhesion by Oral Bacteria. *Annual Review of Microbiology* **50:** 513-512